RELATIVE ORBIT GEOMETRY THROUGH CLASSICAL ORBIT ELEMENT DIFFERENCES

Hanspeter Schaub
Virginia Polytechnic Institute, Blacksburg, VA 24061

Simulated Reprint from

Journal of Guidance, Navigation and Control
Volume 27, Number 5, Sept.–Oct., 2004, Pages 839–848

A publication of the
American Institute of Aeronautics and Astronautics, Inc.
1801 Alexander Bell Drive, Suite 500
Reston, VA 22091

Journal of Guidance, Navigation and Control
Vol. 27, No. 5, Sept. 2004

RELATIVE ORBIT GEOMETRY THROUGH CLASSICAL ORBIT ELEMENT DIFFERENCES

Hanspeter Schaub*
Virginia Polytechnic Institute, Blacksburg, VA 24061

The relative orbit geometry of a spacecraft formation can be elegantly described in terms of a set of orbit element differences relative to a common chief orbit. For the non-perturbed orbit motion these orbit element differences remain constant if the anomaly difference is expressed in terms of the mean anomaly and all semi-major axes are equal. A general method is presented to estimate the linearized relative orbit geometry for both circular and elliptic chief reference orbits. The relative orbit is described purely through relative orbit element differences, not through the classical method of using Cartesian initial conditions. Analytical solutions of the relative motion are provided in terms of the true anomaly angle. By sweeping this angle from 0 to 2π, it is trivial to estimate the along-track, out-of-plane and orbit radial dimensions. The orbit element based relative motion predictions are valid for both the osculating element space and the mean element space. The main assumption being made in the linearization is that the relative orbit radius is small compared to the inertial orbit radius relative to Earth. The resulting linearized relative motion solution can be used to assist in selecting the orbit element differences that yield a natural desired relative orbit geometry. Linearized analytical solutions are provided that show what secular drift is caused by having a non-zero semi-major axis difference, or what influence the J_2 gravitational perturbation will have on the mean relative motion.

Introduction

To describe and control the relative motion between various spacecraft in a formation, various coordinate sets have traditionally been used. A common choice is to use the Cartesian coordinates of the relative position vector with components expressed in the rotating rotating Hill coordinate frame.[1–3] The six Cartesian initial conditions are the invariant parameters of the relative orbit. A more accurate choice in coordinates would be to use curvilinear coordinates in the same Hill coordinate frame. Using either set, assuming a small relative orbit size and a circular chief orbit, it is possible to solve the corresponding Clohessy-Wiltshire differential equations of motion and obtain an analytical expression of all possible uncontrolled relative motions. This solution has been extensively used to study the linearized relative motion of satellites and design reference trajectories for the relative orbit control problem. An alternate set of six invariant parameters to describe the relative orbit is to use orbit element differences relative to the chief orbit.[4–8] Prescribing the relative orbit geometry through sets of relative orbit element differences has the major advantage that these relative orbit coordinates are constants of the non-perturbed orbit motion. Even if perturbations are present, they typically cause the orbit element differences to vary slowly with time.

Several relative orbit control strategies have recently been suggested that feed back relative orbit errors in terms of orbit element differences.[9–13] However, no mention is made in these references how to construct a desired relative orbit geometry using orbit element differences. Typically the required orbit element differences are found through a trial and error method of changing the orbit elements and observing the resulting relative orbit geometry. This is particularly true if the chief orbit has a significant non-zero eccentricity value. In comparison, the analytical relative motion solution of the Clohessy-Wiltshire equations provides direct insight into the shape, size and location of the relative orbit. However, this elegantly simple result is only valid for circular chief orbits.

The goal of this paper is to provide simple linearized estimates of the uncontrolled (x, y, z) relative orbit motion in the rotating Hill frame in terms of classical orbit element differences. Note that the relative motion is still assumed to be defined in terms of the orbit element differences and not the Cartesian coordinates. However, the latter coordinates are used to describe the resulting relative orbit geometry in a more intuitive manner. Contrary to previous work in this area,[7,8] the presented results are general in that they show the effect of all six orbit element differences and apply to both circular and elliptic chief orbits. Direct linearized relationships between the orbit element differences and the resulting relative orbit geometry are presented for both circular and eccentric chief orbits. No small eccentricity assumptions are required in this development. In particular, the relative orbit along-track, out-of-plane and orbit radial motion and offsets are estimated for specific sets of orbit element differences for the case of bounded relative orbits. The only linearizing assumption made here is that the relative orbit radius is small compared to the inertial orbit radius. Further, linear approximations to the orbit element drift equations are provided for having unequal orbit energies and for studying mean relative orbit motion under the J_2 gravitational influence. The solution is valid for both bounded and un-bounded relative motion. However, the relative orbit (x, y, z) description is now only valid as long as the relative orbit radius is small compared to the inertial orbit radius. Note that the orbit element difference description itself is still valid if this is not the case, only the linearized mapping into the (x, y, z) Hill frame coordinates breaks down at this point.

Analytical solutions to the linearized relative motion with eccentric chief orbits have been studied in References 14–20. Melton developed a state transition matrix that can be used to predict the relative motion for chief orbits with small eccentricities.[14] Tschauner and Hempel have solved the relative equations of motion directly for the general case of having an elliptic chief orbit.[15] Kechichian develops in Reference 16 the analytical solution to the relative orbit motion under the influence of both the J_2 and J_3 zonal harmonics assuming that the eccentricity is a very small parameter. However, all these relative motion solutions are not explicit and require the computation of an integral. In Reference 17 Carter does present an analytical solution to the linearized relative motion where the true anomaly is used as the independent variable. However, this solution is in terms of the Cartesian coordinates and not in terms of the desired orbit element differences. Reference 20 uses this analytical linearized motion result from Carter to study the relative motion dynamics of elliptic chief orbits and derives Cartesian Hill frame coordinate conditions for bounded relative motion. More recently, Broucke has presented in Reference 19 an analytical solution to the linearized relative equations of motion for eccentric chief orbits. His solution uses both time and true anomaly and finds the current Cartesian coordinates of a deputy satellite given the initial Cartesian coordinates. Unfortunately all these methods yield relatively complex solutions and the six Cartesian relative motion initial conditions do not easily reveal the

*Assistant Professor, Senior AIAA Member.

geometry of the resulting relative orbit. In particular, the secular and sinusoidal contributions are not easily separated as is the case with the CW equations solution. Thus, it is not intuitive to the relative orbit design process how to adjust the initial Cartesian conditions to obtain a relative orbit of the desired shape and size without resorting to a numerical trial and error method.

In References 12 and 21, a linearized mapping is presented between a particular set of orbit element differences and the Cartesian position and velocity coordinates in the rotating Hill reference frame. This work was then expanded in Reference 18 to provide the state transition matrix for the relative orbit motion using a set of orbit elements which are non-singular for circular orbits. In the present paper the linearized mapping in Reference 12 between orbit element differences and the rotating Cartesian coordinates is recast into a new form using the classical orbit elements. The simpler result can describe the relative orbit geometry (i.e. relative orbit positions) without singularities, thus there is no need to use the mathematically more complex non-singular orbit elements. Further, the solution is presented in terms of differences in mean anomalies and not differences in true latitude angles as in Reference 12. The reason being that for elliptic motions, a mean anomaly difference between two satellites remains constant under the assumption of classical Keplerian motion and equal orbit energies. The final relative motion description is then simplified to a form which isolates the static offsets and the sinusoidal motion components, analogous to the algebraic form of the analytical solution of the Clohessy-Wiltshire equations. The resulting linearized analytic relative orbit solution is useful when designing a relative orbit that must meet scientific mission requirements. If the relative orbit must have a certain along-track behavior, then this solution directly shows how to adjust the relative orbit element differences to achieve the desired motion. Further, the general solution for elliptic chief orbits is specialized for the small eccentricity case and near circular orbit case.

Note that this paper does not discuss control applications of this linearized relative motion description. This requires developing the relative orbit velocity expressions. Reference 12 illustrates how the complete linearized mapping between non-singular orbit element differences and Cartesian Hill frame coordinates, including velocity expressions, can be combined in a hybrid control law. Instead, the relative motion equations in this paper are provided for analysis purposes to study natural, uncontrolled relative motions.

Relative Orbit Definitions

The following nomenclature is adopted to describe the satellites within a spacecraft formation. The satellite about which all other satellites are orbiting is referred to as the chief satellite. The remaining satellites, referred to as the deputy satellites, are to fly in formation with the chief. Note that it is not necessary that the chief position actually be occupied by a physical satellite. Sometimes this chief position is simply used as an orbiting reference point about which the deputy satellites orbit. To express how the relative orbit geometry is seen by the chief, we introduce the Hill coordinate frame $\mathcal{O}$.[22] Its origin is at the osculating chief satellite position and its orientation is given by the vector triad $\{\hat{\boldsymbol{o}}_r, \hat{\boldsymbol{o}}_\theta, \hat{\boldsymbol{o}}_h\}$ shown in Figures 1. The unit vector $\hat{\boldsymbol{o}}_r$ is in the orbit radius direction, while $\hat{\boldsymbol{o}}_h$ is parallel to the orbit momentum vector in the orbit normal direction. The unit vector $\hat{\boldsymbol{o}}_\theta$ then completes the right-handed coordinate system. Let $\boldsymbol{r}$ be the chief orbit radius and $\boldsymbol{h}$ be the chief angular momentum vector. Unless noted otherwise, any non-differenced states or orbit elements are assumed to be those of the chief. Differenced states are assumed to be differences between the deputy and chief satellite. Mathematically, these $\mathcal{O}$ frame orientation vectors are expressed as

$$\hat{\boldsymbol{o}}_r = \frac{\boldsymbol{r}}{r} \tag{1a}$$

$$\hat{\boldsymbol{o}}_\theta = \hat{\boldsymbol{o}}_h \times \hat{\boldsymbol{o}}_r \tag{1b}$$

$$\hat{\boldsymbol{o}}_h = \frac{\boldsymbol{h}}{h} \tag{1c}$$

with $\boldsymbol{h} = \boldsymbol{r} \times \dot{\boldsymbol{r}}$. Note that if the inertial chief orbit is circular, then $\hat{\boldsymbol{o}}_\theta$ is parallel to the satellite velocity vector.

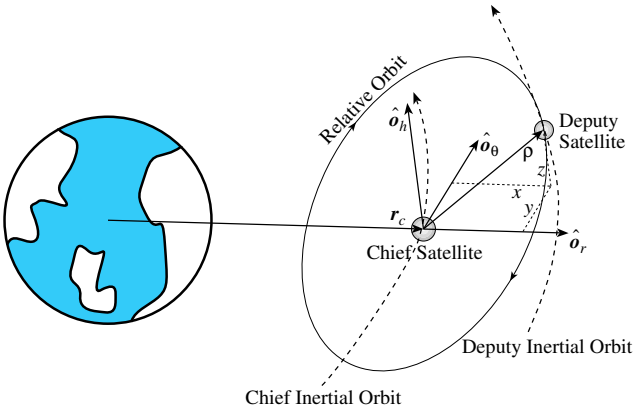

Fig. 1 Illustration of a General Type of Spacecraft Formation with Out-Of-Plane Relative Motion

The relative orbit position vector $\boldsymbol{\rho}$ and velocity vector $\dot{\boldsymbol{\rho}}$ of a deputy satellite relative to the chief is expressed in Cartesian $\mathcal{O}$ frame components as

$$\boldsymbol{\rho} = (x, y, z)^T \tag{2}$$

$$\dot{\boldsymbol{\rho}} = (\dot{x}, \dot{y}, \dot{z})^T \tag{3}$$

The relative position and velocity vectors are compactly written as

$$\boldsymbol{X} = \begin{pmatrix} \boldsymbol{\rho} \\ \dot{\boldsymbol{\rho}} \end{pmatrix} \tag{4}$$

Thus, given both the relative position vector $\boldsymbol{\rho}$ and the chief position vector $\boldsymbol{r}$, we are able to determine the inertial motion of a deputy satellite. Note that the x and y coordinates don't have to be interpreted as rectilinear coordinates. Interpreting them as curvilinear coordinates no changes in the mathematical expressions are required. Here x is interpreted as a difference in the orbit radius and y is interpreted as the curved flight path difference. Assuming x and y are curvilinear results greatly enhances the accuracy of the linearization result.

Instead of using Cartesian coordinates to describe the relative position of a deputy to the chief, we can also use orbit element differences.[4,5] Let the vector $\boldsymbol{e}$ be defined through the orbit elements

$$\boldsymbol{e} = (a, \theta, i, q_1, q_2, \Omega)^T \tag{5}$$

where a is the semi-major axis, $\theta = \omega + f$ is the true latitude angle, i is the orbit inclination angle, Ω is the argument of the ascending node and q_i are defined as

$$q_1 = e\cos\omega \tag{6}$$

$$q_2 = e\sin\omega \tag{7}$$

The parameter e is the eccentricity, ω is the argument of perigee, and f be the true anomaly. Let the relative orbit be described through the orbit element difference vector $\delta\boldsymbol{e}$. Whereas all six elements of the relative orbit state $\boldsymbol{X}$ vector are time varying, all the orbit element differences, except for the true anomaly difference, are constant for a non-perturbed Keplerian orbit. This has many advantages

when measuring the relative orbit error motion and applying it to a control law. In References 21 and 12 a convenient direct mapping is presented which translates between the Cartesian states $\boldsymbol{X}$ and the orbit element differences $\delta\boldsymbol{e}$. In deriving this mapping, it is assumed that the relative orbit radius ρ is small in comparison to the inertial chief orbit radius r. While Reference 12 shows both the forward and backward mapping between these relative orbit coordinates, only the mapping from orbit element differences to Cartesian Hill frame coordinates is used in the following development. The relative position vector components are given in terms of orbit elements through:

$$\begin{aligned} x \approx & \frac{r}{a}\delta a + \frac{V_r}{V_t} r\ \delta\theta - \frac{r}{p}(2aq_1 + r\cos\theta)\delta q_1 \\ & - \frac{r}{p}(2aq_2 + r\sin\theta)\delta q_2 \end{aligned} \tag{8a}$$

$$y \approx r(\delta\theta + \cos i\ \delta\Omega) \tag{8b}$$

$$z \approx r(\sin\theta\ \delta i - \cos\theta\sin i\ \delta\Omega) \tag{8c}$$

The parameter $p = a(1-e^2) = a\eta^2$ is the semi-latus rectum, with $\eta = \sqrt{1-e^2}$ being another convenient measure of the orbit eccentricity. The chief radial and transverse velocity components V_r and V_t are defined as

$$V_r = \dot{r} = \frac{h}{p}(q_1\sin\theta - q_2\cos\theta) \tag{9}$$

$$V_t = r\dot{\theta} = \frac{h}{p}(1 + q_1\cos\theta + q_2\sin\theta) \tag{10}$$

The orbit radius r is defined in terms of the orbit elements used in Eq. (5) as

$$r = \frac{a(1-q_1^2-q_2^2)}{1 + q_1\cos\theta + q_2\sin\theta} = \frac{a\eta^2}{1 + e\cos f} \tag{11}$$

Note that the ratio V_r/V_t in Eq. (8a) can be rewritten as

$$\frac{V_r}{V_t} = \frac{q_1\sin\theta - q_2\cos\theta}{1 + q_1\cos\theta + q_2\sin\theta} = \frac{e\sin f}{1 + e\cos f} \tag{12}$$

Alternate mappings between orbit element differences and Cartesian relative orbit coordinates are found in References 6 and 23. The following development will take this orbit element mapping between local Cartesian coordinates and orbit element differences and reformulate the solution into a new form where the relative orbit geometry will be readily apparent. For the circular chief orbit special case, the Hill or Clohessy-Wiltshire (CW) relative equations of motion have the convenient analytical solution[24,25]

$$x(t) = A_0\cos(nt + \alpha) + x_{\text{off}} \tag{13a}$$

$$y(t) = -2A_0\sin(nt + \alpha) + y_{\text{off}} - \frac{3}{2}nx_{\text{off}}t \tag{13b}$$

$$z(t) = B_0\cos(nt + \beta) \tag{13c}$$

The integration constants A_0, B_0, α, β, x_{off} and y_{off} are determined through the relative orbit initial conditions. By choosing the initial relative orbit Cartesian coordinates, the resulting relative orbit geometry can be easily seen through the secular, sinusoidal and constant terms in Eq. (13). For the relative orbit designer, what classes of unforced relative orbit motion is possible is readily apparent. This type of relative orbit geometry analysis is not possible with the form of the relative motion description in Eq. (8), because the terms $\delta\theta$, r, V_r and V_θ are all time varying. The following development will yield a simple solution of the linearized relative motion for generally eccentric orbits that is equivalent to the simple classical CW solution of the circular chief motion special case. Given specified orbit element differences, the resulting linearized relative orbit motion will be seen through a simple combination of constant offsets, secular terms, and sinusoidal components. Contrary to the CW analytical solution, this relative orbit description will apply to both circular and eccentric chief orbits.

Mean Anomaly Drift Due to Unequal Orbit Energies

Assuming unperturbed Keplerian motion, the orbit period is determined solely from the semi-major axis a. Ignoring other perturbations, if two orbits have unequal semi-major axes, then we expect the two anomaly angles to drift apart. Thus, having a non-zero δa will result in the mean anomaly difference δM having a secular drift. This section derives analytical solutions the mean anomaly drift in terms of the true anomaly angle as the independent variable instead of the time variable. These first order approximations will be of use in the following sections where the linearized relative motion is described in terms of mean anomaly differences. The chief mean anomaly M is given by

$$M(t) = nt + M_0 = \sqrt{\frac{\mu}{a^3}}t + M_0 \tag{14}$$

where $M_0 = M(t_0)$. The mean anomaly rate is expressed as

$$\dot{M} = \frac{\mathrm{d}M}{\mathrm{d}t} = \sqrt{\frac{\mu}{a^3}} \tag{15}$$

Taking the first variation of Eq. (15), we find that small differences in mean anomaly rates $\delta\dot{M}$ are related to small differences in the semi-major axis δa through

$$\delta\dot{M} = \frac{\mathrm{d}(\delta M)}{\mathrm{d}t} = -\frac{3}{2}\sqrt{\frac{\mu}{a^5}}\delta a = -\frac{3}{2}n\frac{\delta a}{a} \tag{16}$$

By defining these differences to be differences between deputy and chief satellite orbit elements, Eq. (16) provides an approximation to how the mean anomaly difference will vary due to δa. Note that the true nonlinear drift in mean anomalies is given by

$$\delta\dot{M} = \dot{M}_d - \dot{M} = \sqrt{\frac{\mu}{(a+\delta a)^3}} - \sqrt{\frac{\mu}{a^3}} \tag{17}$$

where $a_d = a + \delta a$. We could easily integrate Eq. (16) with respect to time to estimate the mean anomaly difference at a particular time step t. However, it would still be necessary to solve Kepler's equation to relate a time t to the corresponding true anomaly angle f to make use of the relative orbit description in terms of true anomaly dependent orbit element differences. These are extra steps in evaluating the linearized relative orbit that are preferably avoided in order to yield a simple analytical solution of the linearized relative motion applicable for relative motion analysis. The following steps will lead to an analytical solution of the linearized drift equation $\delta\dot{M}(f)$. First the differential equation in Eq. (16), which is expressed with respect to time, is rewritten to be expressed with respect to the true anomaly f. To accomplish this, we make use of the identity

$$\frac{\mathrm{d}t}{\mathrm{d}f} = \frac{r^2}{h} = \frac{\eta^3}{n(1 + e\cos f)^2} \tag{18}$$

where $\eta = \sqrt{1-e^2}$. Multiplying both sides of Eq. (16) by $\mathrm{d}t/\mathrm{d}f$, we find

$$\delta M' = \frac{\mathrm{d}}{\mathrm{d}f}(\delta M) = -\frac{3}{2}\frac{\eta^3}{(1 + e\cos f)^2}\frac{\delta a}{a} \tag{19}$$

The differential equation in Eq. (19) could be numerically integrated with respect to the true anomaly f to find the required $\delta M(f)$ without having to solve Kepler's equation at each integration step. However, this differential equation can be solved analytically as well. Note that

$$\int_{f_0}^{f} \frac{\eta^3}{(1 + e\cos f)^2}\mathrm{d}f = M(f) - M_0 \tag{20}$$

where $M_0 = M(f_0)$. Applying this integral solution to Eq. (19) yields:

$$\delta M(f) = \delta M_0 - \frac{3}{2}\left(M(f) - M_0\right)\frac{\delta a}{a} \tag{21}$$

The mean anomaly is expressed in terms of the true anomaly using

$$M = E(f) - e\sin E(f) \tag{22}$$

The variable E is the eccentric anomaly and is related to the true anomaly f through the transformation

$$E(f) = 2\arctan\left(\frac{\sqrt{1-e}\sin(f/2)}{\sqrt{1+e}\cos(f/2)}\right) \tag{23}$$

When numerically evaluating $E(f)$, note that the `atan2(x,y)` function should be used to avoid arctan() singularities and obtain angles in the proper quadrant. Thus, Eq. (21) provides a direct analytical approximation of the mean anomaly drift due to δa in terms of the true anomaly f. Further, note that this $\delta M(f)$ approximation is valid for chief orbits of any eccentricity, as long as the relative orbit size has not grown large compared to the chief inertial orbit radius. The term $M(f)$ provides the expected secular term in $\delta M(f)$ due to the semi-major axis difference δa and will grow unbounded with time.

A common mission scenario is that the chief orbit only has a weakly eccentric orbit. The general expression in Eq. (21) can then be refined by neglecting higher order terms of the eccentricity e and only retaining terms which are linear in e. Since we are already dropping higher order terms in ρ/r to obtain the linearized relative motion equations, a weakly eccentric orbit is understood to be one where e^n (with $n > 1$) is smaller than ρ/r and e is larger than ρ/r. For this case, the approximation of the mean anomaly drift $\delta M(f)$ is expressed as

$$\delta M(f) = \delta M(f_0) - \frac{3}{2}\left(f - 2e\sin f\right)\Big|_{f_0}^{f}\frac{\delta a}{a} \tag{24}$$

If the chief orbit is essentially circular, then e is virtually zero and much smaller than the relative orbit radius to inertial orbit radius ratio ρ/r. In this case, the approximation of the mean anomaly drifts $\delta M(f)$ is reduced to

$$\delta M(f) = \delta M(f_0) - \frac{3}{2}\left(f - f_0\right)\frac{\delta a}{a} \tag{25}$$

General Elliptic Orbits

To find a simple closed-form analytical solution of the linearized relative motion, note that Eq. 8 provides a direct linear mapping between orbit element differences $\delta\boldsymbol{e}$ and the Hill frame Cartesian coordinates $\boldsymbol{\rho}$. The only linearizing assumption made is that the relative orbit radius ρ is small compared to the inertial chief orbit radius r. No small eccentricity assumptions have been made. However, when describing a relative orbit through orbit element differences, it is not convenient to describe the anomaly difference through $\delta\theta$ or δf. For elliptic chief orbits, the difference in true anomaly between two orbits will vary with time even when the relative orbit is closed and bounded. To avoid this issue, the desired anomaly difference between two orbits is expressed here in terms of a mean anomaly difference δM. This anomaly difference will remain constant even for elliptic chief orbits, assuming unperturbed Keplerian motion with equal orbit energy states as shown in Eqs. (21), (24) and (25). To express the mean anomaly differences in terms of other anomaly differences, we make use of the mean anomaly definition

$$M = E - e\sin E \tag{26}$$

where E is the eccentric anomaly. Taking its first variation we express differences in mean anomaly in terms of differences in eccentric anomaly and differences in eccentricity.

$$\begin{aligned}\delta M &= \frac{\partial M}{\partial E}\delta E + \frac{\partial M}{\partial e}\delta e \\ &= (1 - e\cos E)\delta E - \sin E\delta e\end{aligned} \tag{27}$$

Using the mapping between eccentric anomaly E and true anomaly f

$$\tan\frac{f}{2} = \sqrt{\frac{1+e}{1-e}}\tan\frac{E}{2} \tag{28}$$

and taking its first variation, differences in E are then expressed as differences in f and e through

$$\delta E = \frac{\eta}{1+e\cos f}\delta f - \frac{\sin f}{1+e\cos f}\frac{\delta e}{\eta} \tag{29}$$

Substituting Eq. (29) into Eq. (27) and making use of the orbit identities

$$(1 - e\cos E) = \frac{\eta^2}{(1+e\cos f)} \tag{30}$$

$$\sin E = \frac{\eta\sin f}{(1+e\cos f)} \tag{31}$$

the desired relationship between differences in true and mean anomalies is found.

$$\delta f = \frac{(1+e\cos f)^2}{\eta^3}\delta M + \frac{\sin f}{\eta^2}(2 + e\cos f)\delta e \tag{32}$$

Let us redefine the orbit element difference vector $\delta\boldsymbol{e}$ to consist of the classical orbit elements:

$$\delta\boldsymbol{e} = (\delta a, \delta M, \delta i, \delta\omega, \delta e, \delta\Omega)^T \tag{33}$$

Note that all these orbit element differences are constants for Keplerian two-body motion where all orbits have equal energy states. Further, while using q_1 and q_2 instead of e and ω allows us to avoid singularity issues for near-circular orbit velocity expressions, for the following relative orbit geometry discussion such singularities do not appear. In fact, describing the relative orbit path using δe and $\delta\omega$ instead of δq_1 and δq_2 yields a simpler, more elegant, and thus a more intuitive result to analyze all possible unforced relative orbits. However, to use this linear mapping between orbit element differences and Hill frame Cartesian coordinates in control applications, the non-singular elements in Eq. (5) should be used to avoid near-circular orbit singularity issues. Control laws using Eq. (8) have been discussed in Reference 12. Using Eqs. (6) and (7), the differences in the q_i parameters are expressed as

$$\delta q_1 = \cos\omega\delta e - e\sin\omega\delta\omega \tag{34a}$$

$$\delta q_2 = \sin\omega\delta e + e\cos\omega\delta\omega \tag{34b}$$

After substituting Eqs. (32) and (34) into the linear mapping in Eq. (8) and simplifying the result, we are able to express the relative position coordinates (x, y, z) in terms of the orbit element differences in Eq. (33) through

$$x(f) \approx \frac{r}{a}\delta a + \frac{ae\sin f}{\eta}\delta M - a\cos f\delta e \tag{35a}$$

$$\begin{aligned}y(f) \approx{}& \frac{r}{\eta^3}(1+e\cos f)^2\delta M + r\delta\omega \\ &+ \frac{r\sin f}{\eta^2}(2 + e\cos f)\delta e + r\cos i\delta\Omega\end{aligned} \tag{35b}$$

$$z(f) \approx r(\sin\theta\delta i - \cos\theta\sin i\delta\Omega) \tag{35c}$$

Note that with this linearized mapping the difference in the argument of perigee $\delta\omega$ does not appear in the $x(f)$ expression. Further, these equations are valid for both circular and elliptic chief orbits. Only the δM and δe terms contribute periodic terms to the radial $x(f)$ solution. Due to the dependence of r on the true anomaly f, all orbit element difference terms in the along-track $y(f)$ motion contribute both static offsets as well as periodic terms. For the out-of-plane $z(f)$ motion both the δi and $\delta\Omega$ terms control the out-of-plane oscillations. By dividing the dimensional (x, y, z) expressions in Eq. (35) by the chief orbit radius $r(f)$ and making use of Eq. (11), we obtain the non-dimensional relative orbit coordinates (u, v, w).

$$\begin{aligned}\frac{x(f)}{r(f)} = u(f) \approx \frac{\delta a}{a} + (1+e\cos f)\frac{e\sin f}{\eta^3}\delta M \\ - \frac{(1+e\cos f)}{\eta^2}\cos f\delta e\end{aligned} \tag{36a}$$

$$\begin{aligned}\frac{y(f)}{r(f)} = v(f) \approx (1+e\cos f)^2\frac{\delta M}{\eta^3} + \delta\omega \\ + \frac{\sin f}{\eta^2}(2+e\cos f)\delta e + \cos i\delta\Omega\end{aligned} \tag{36b}$$

$$\frac{z(f)}{r(f)} = w(f) \approx \sin\theta\delta i - \cos\theta\sin i\delta\Omega \tag{36c}$$

Since $(y, z) \ll r$, the non-dimensional coordinates (v, w) are the angular deputy satellite relative orbit position with respect to the chief orbit radius axis.

However, the present form of Eq. (36) is not convenient to determine the overall non-dimensional shape of the relative orbit. The reason is that there are several sin() and cos() functions being added here. Using the identities

$$\begin{aligned}A\sin t + B\cos t &= \sqrt{A^2+B^2}\cos\left(t - \tan^{-1}\left(\frac{A}{B}\right)\right) \\ &= -\sqrt{A^2+B^2}\sin\left(t - \tan^{-1}\left(\frac{B}{-A}\right)\right)\end{aligned} \tag{37}$$

as well as standard trigonometric identities, we are able to rewrite the linearized non-dimensional relative orbit motion as

$$\begin{aligned}u(f) \approx \frac{\delta a}{a} + \frac{1}{\eta^2}\sqrt{\frac{e^2\delta M^2}{\eta^2} + \delta e^2}\cos(f - f_u) \\ - \frac{e\delta e}{2\eta^2} + \frac{e}{2\eta^2}\sqrt{\frac{e^2\delta M^2}{\eta^2} + \delta e^2}\cos(2f - f_u)\end{aligned} \tag{38a}$$

$$\begin{aligned}v(f) \approx \left(\left(1+\frac{e^2}{2}\right)\frac{\delta M}{\eta^3} + \delta\omega + \cos i\delta\Omega\right) \\ + \frac{2}{\eta^2}\sqrt{\frac{e^2\delta M^2}{\eta^2} + \delta e^2}\cos(f - f_v) \\ + \frac{e}{2\eta^2}\sqrt{\frac{e^2\delta M^2}{\eta^2} + \delta e^2}\cos(2f - f_v)\end{aligned} \tag{38b}$$

$$w(f) \approx \sqrt{\delta i^2 + \sin^2 i\,\delta\Omega^2}\cos(\theta - \theta_w) \tag{38c}$$

with the phase angles f_u, f_v and θ_w being defined as

$$f_u = \tan^{-1}\left(\frac{e\delta M}{-\eta\delta e}\right) \tag{39a}$$

$$f_v = \tan^{-1}\left(\frac{\eta\delta e}{e\delta M}\right) = f_u - \frac{\pi}{2} \tag{39b}$$

$$\theta_w = \tan^{-1}\left(\frac{\delta i}{-\sin i\ \delta\Omega}\right) \tag{39c}$$

At the phase angles f_u and θ_w, the trigonometric terms will reach either their minimum or maximum value. Note that 180 degrees can be added or subtracted from these angles to yield the second extrema point of the trigonometric functions. To further reduce the expression in Eq. (38), let us introduce the small states δ_u and δ_w:

$$\delta_u = \sqrt{\frac{e^2\delta M^2}{\eta^2} + \delta e^2} \tag{40a}$$

$$\delta_w = \sqrt{\delta i^2 + \sin^2 i\,\delta\Omega^2} \tag{40b}$$

Using these δ_u and δ_w definitions as well as Eq. (39b), the linearized relative orbit motion is described through

$$\begin{aligned}u(f) \approx \frac{\delta a}{a} - \frac{e\delta e}{2\eta^2} \\ + \frac{\delta_u}{\eta^2}\left(\cos(f - f_u) + \frac{e}{2}\cos(2f - f_u)\right)\end{aligned} \tag{41a}$$

$$\begin{aligned}v(f) \approx \left(\left(1+\frac{e^2}{2}\right)\frac{\delta M}{\eta^3} + \delta\omega + \cos i\delta\Omega\right) \\ - \frac{\delta_u}{\eta^2}\left(2\sin(f - f_u) + \frac{e}{2}\sin(2f - f_u)\right)\end{aligned} \tag{41b}$$

$$w(f) \approx \delta_w\cos(\theta - \theta_w) \tag{41c}$$

These equations describe the general linearized relative motion of the deputy satellite relative to the chief in terms of orbit element differences and using true anomaly as the independent variable. For the non-dimensional motion where $\delta a = 0$ and $\delta M =$ constant, static offsets terms and sinusoidal terms are cleanly separated as is the case with the classical analytical relative motion solution of the CW equations in Eq. (13). The secular growth terms are hidden in the orbit element description in the orbit element differences themselves. For this common analytical case where feasible bounded relative motions are studied, the relative motion is obtained using Eq. (41) by simply sweeping the true anomaly angle from its initial state $f(t_0)$ to its final state $f(t_f)$. For the case where a nonzero δa is considered, then Eq. (21) is used to express the now time dependent $\delta M(f)$ term. If the orbit element differences vary with time due non-Keplerian influences, then the orbit element drift differential equation $\delta\dot{\boldsymbol{e}}$ will have to be solved numerically for the most general case. To relate the anomaly angle and the current time, Kepler's equation must be solved at each time step.

To avoid standard inverse tangent singularities in the computation of the phase angles in Eqs. (39a) – (39c), it is important that the `atan2(x,y)` function and not the `atan(x)` function is used to obtain an angle in the proper quadrant. The only numerical problems that might arise computing f_u or f_v is when either e or δM and δe are zero. For this degenerate case there would be no relative in-plane motion between the deputy and chief satellites ($\delta_u = 0$) and the phase angle f_u is arbitrary. However, typical relative orbit designs require a non-zero δe or δM term. Similarly, the θ_w angle is arbitrary if either i or $\delta\Omega$ and δi are zero. However, in this degenerate case no relative out-of-plane motion would occur with δ_w being zero.

Note that the $\cos(2f)$ and $\sin(2f)$ terms are multiplied by the eccentricity e. Only if the chief orbit is very eccentric will these terms have a significant contribution to the overall relative orbit dimension. For the more typical case of having a chief orbit with a small eccentricity e, these terms only provide small perturbations to the dominant $\sin(f)$ and $\cos(f)$ terms. However, the linearized relative motion solution shown is valid for any elliptic chief orbit eccentricity. No expansions in e have been taken here. Using Eq. (41), it is trivial to determine the maximum radial, along-track and out-of-plane dimension of a relative orbit provided that the relative orbit geometry is prescribed through the set of orbit element differences $\{\delta a, \delta e, \delta i, \delta\Omega, \delta\omega, \delta M\}$. The only linearizing assumption made so far is that the relative orbit radius is small compared to the planet centric inertial orbit

radius. However, note that we are only estimating the non-dimensional relative orbit shape. To obtain the true radial, along-track and out-of-plane motions, we need to multiply (u, v, w) by the chief orbit radius r. Since r is time dependent for an elliptic chief orbit, the points of maximum angular separation between deputy and chief satellites may not correspond to the point of maximum physical distance. To plot the dimensional linearized relative orbit motion, we use Eq. (35) instead. However, due to the ratio's of sin() and cos() terms, it is not trivial to obtain the maximum physical dimensions of the relative orbit.

Let us take a closer look at the out-of-plane motion. The true latitude angle θ_w, at which the maximum angular out-of-plane motion will occur, is given by Eq. (39c). As expected, if only a $\delta\Omega$ is prescribed, then the maximum $w(f)$ motion occurs during the equator crossing at $\theta = 0$ or 180 degrees. If only a δi is prescribed, then the maximum w motion occurs at $\theta = \pm 90$ degrees.

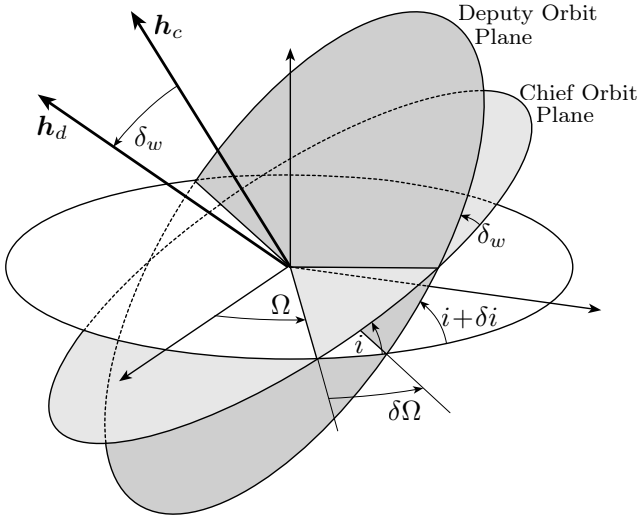

Fig. 2 Illustration of Orbit Plane Orientation Difference between Chief and Deputy Satellites

The maximum angular out-of-plane motion is given by the angle δ_w as shown in Figure 2. This angle δ_w is the tilt angle of the deputy orbit plane relative to the chief orbit plane. As such, it is the angle between the angular momentum vector of the chief orbit and the angular momentum vector of the deputy orbit. To prove that δ_w is indeed this angle, let us make use of the spherical law of cosines for angles. Using the spherical trigonometric law of cosines, we are able to relate the angles $\delta\Omega$, i, δi and δ_w through:[26]

$$\cos\delta_w = \cos i\cos(i+\delta i) + \sin i\sin(i+\delta i)\cos\delta\Omega \tag{42}$$

Assuming that $\delta\Omega$, δi and δ_w are small angles, we approximate $\sin x \approx x$ and $\cos x \approx 1 - x^2/2$ to solve for δ_w.

$$\delta_w = \sqrt{\delta i^2 + \sin^2 i\delta\Omega^2} \tag{43}$$

Using the angle δ_w, the out-of-plane motion $w(f)$ in Eq. (41c) is written in the compact form shown.[8,27]

Chief Orbits with Small Eccentricity

In this section we assume that the chief orbit eccentricity e is a small quantity. In particular, we assume that e is small but greater than ρ/r, while powers of e are smaller than ρ/r and are thus dropped. The inertial orbit radius r is now approximated as

$$r = \frac{a\eta^2}{1+e\cos f} \approx a(1-e\cos f) \tag{44}$$

while $\eta^2 \approx 1$. The linearized dimensional relative orbit motion in Eq. (35) is written for the small eccentricity case as:

$$x(f) \approx (1-e\cos f)\delta a + \frac{ae\sin f}{\eta}\delta M - a\cos f\delta e \tag{45a}$$

$$y(f) \approx \frac{a}{\eta}(1+e\cos f)\delta M + a(1-e\cos f)\delta\omega + a\sin f(2-e\cos f)\delta e + a(1-e\cos f)\cos i\delta\Omega \tag{45b}$$

$$z(f) \approx a(1-e\cos f)(\sin\theta\delta i - \cos\theta\sin i\delta\Omega) \tag{45c}$$

Making use of the trigonometric identity in Eq. (37), the (x, y, z) motion is re-written as

$$x(f) \approx \delta a + a\delta_x\cos(f - f_x) \tag{46a}$$

$$y(f) \approx a\left(\frac{\delta M}{\eta} + \delta\omega + \cos i\delta\Omega\right) - a\delta_y\sin(f - f_y) - \frac{ae}{2}\sin(2f)\delta e \tag{46b}$$

$$z(f) \approx a\delta_z\cos(\theta - \theta_z) - \frac{ae}{2}\delta_z\cos(2f - f_z) - \frac{ae}{2}(\sin\omega\delta i - \cos\omega\sin i\delta\Omega) \tag{46c}$$

with the small states δ_x, δ_y and δ_z being defined as

$$\delta_x = \sqrt{\frac{e^2\delta M^2}{\eta^2} + \left(\delta e + \frac{\delta a}{a}\right)^2} \tag{47a}$$

$$\delta_y = \sqrt{4\delta e^2 + e^2\left(\frac{\delta M}{\eta} - \delta\omega - \cos i\delta\Omega\right)^2} \tag{47b}$$

$$\delta_z = \sqrt{\delta i^2 + \sin^2 i\delta\Omega^2} \tag{47c}$$

and the phase angles f_x, f_y, θ_z and f_z being defined as

$$f_x = \tan^{-1}\left(\frac{e\delta M}{-\eta\left(\delta e + \frac{\delta a}{a}\right)}\right) \tag{48a}$$

$$f_y = \tan^{-1}\left(\frac{e\left(\frac{\delta M}{\eta} - \delta\omega - \cos i\delta\Omega\right)}{-2\delta e}\right) \tag{48b}$$

$$\theta_z = \tan^{-1}\left(\frac{\delta i}{-\sin i\delta\Omega}\right) \tag{48c}$$

$$f_z = \tan^{-1}\left(\frac{\cos\omega\delta i + \sin\omega\sin i\delta\Omega}{\sin\omega\delta i - \cos\omega\sin i\delta\Omega}\right) \tag{48d}$$

As was the case for the general eccentric orbit case the linearized relative motion solution in Eq. (46) has the static and trigonometric terms separated. If δa is non-zero, then the $\delta M(f)$ term expressed in Eq. (24) will lead to a secular growth of the relative orbit.

The $\tan^{-1}()$ terms are again computed using the `atan2(x,y)` function to avoid singularities with a zero denominator and obtain an angle in the proper quadrant. Note that the orbital radial motion $x(f)$ for the small eccentricity case is identical to the general orbit radial coordinate in Eq. (35a) if δa is zero. The semi-major axis difference must be zero for bounded relative motion if no perturbations are present. With perturbations present, δa may be non-zero and the orbit radial coordinate will then be different between the linearizing approximations. The estimated along-track motion $y(f)$ and out-of-plane motion $z(f)$ will always be numerically different between the generally elliptic case and the small eccentricity case.

The dimensional form of the relative orbit motion in Eq. (45) is convenient to determine the amplitudes of the sinusoidal motion in either the along-track, orbit radial or out-of-plane motion. Note that since e is considered small,

the double-orbit frequency terms $\sin(2f)$ are only a minor perturbation to the dominant orbit frequency sinusoidal terms. Also, if the orbit element differences remain constant, then the true anomaly angle f determines the relative motion. If $\delta\dot{\boldsymbol{e}}$ is non-zero, then the orbit element drift equations must be solved as well.

Near-Circular Chief Orbit

If the chief orbit is circular or near-circular, and the relative orbit radius is small compared to the planet centric orbit radius, then the linearized relative equations of motion are given through the famous Clohessy-Wiltshire or CW equations.[24] These are sometimes also referred to as Hill's equations.[22] These differential equations of the relative orbit motion can be solved for the explicit analytical solution repeated here.

$$x(t) = A_0\cos(nt+\alpha) + x_{\rm off} \tag{49a}$$

$$y(t) = -2A_0\sin(nt+\alpha) + y_{\rm off} - \frac{3}{2}nx_{\rm off}t \tag{49b}$$

$$z(t) = B_0\cos(nt+\beta) \tag{49c}$$

The integration constants A_0, B_0, α, β, $y_{\rm off}$ and $x_{\rm off}$ are determined through the relative orbit initial conditions. These equations have been extensively used to generate relative orbits if the chief orbit is circular. Let us now compare the predicted (x,y,z) motion in terms of the true anomaly in Eq. (46) to the CW solution in Eq. (49) if the chief orbit is assumed to be near-circular (i.e. $e \ll \rho/r$). In this case terms containing the eccentricity e are dropped, as compared to the small eccentricity case studied earlier where only higher order terms of e were dropped. Assuming that all $\delta\boldsymbol{e}$ components are small (i.e. the relative orbit radius is assumed to be small compared to the inertial orbit radius), and letting $e \to 0$, we find that $r \to a$ and $\eta \to 1$. Further, note that f_x and f_y approach π. Using Eq. (46) and Eq. (25), the relative orbit motion $(x(f), y(f), z(f))$ is expressed for the near-circular chief orbit special case as

$$x(f) \approx a\cos f\delta e + \delta a \tag{50a}$$

$$y(f) \approx -2a\sin f\delta e + a(\delta\omega + \delta M(f_0) + \cos i\delta\Omega) - \frac{3}{2}(f-f_0)\delta a \tag{50b}$$

$$z(f) \approx a\sqrt{\delta i^2 + \sin^2 i\delta\Omega^2}\cos(\theta-\theta_z) \tag{50c}$$

Note that the maximum width of the oscillatory along-track motion y is given by $2a\delta e$. This particular result has been previously presented in References 7 and 8. Comparing Eqs. (49) and (50) and noting that $nt = f - f_0$ for this case, we are able to establish a direct relationship between the CW constants and the orbit element differences.

$$A_0 = a\delta e \tag{51a}$$

$$B_0 = a\sqrt{\delta i^2 + \sin^2 i\delta\Omega^2} \tag{51b}$$

$$\alpha = f_0 \pm \pi \tag{51c}$$

$$\beta = f_0 + \omega - \theta_z \tag{51d}$$

$$x_{\rm off} = \delta a \tag{51e}$$

$$y_{\rm off} = a(\delta\omega + \delta M(f_0) + \cos i\delta\Omega) \tag{51f}$$

Incorporating the J_2 Perturbation

For low Earth orbits (LEO), the J_2 gravitational perturbation is the dominant perturbation for a formation with spacecraft of equal type and build. While the atmospheric drag will cause all satellite orbits to continuously loose energy, the deceleration is nearly identical among these spacecraft. The J_2 perturbation will cause all six orbit elements, and thus all six orbit element differences used to describe the relative orbit, to vary with time. This perturbed motion of the orbit elements is separated into short-period, long-period and secular motion.[28] The short and long period motion is cyclic and does not cause unbounded relative orbit grow. The instantaneous motion of a satellite is referred to as the osculating motion. The mean motion is what remains after the short period and long period motions have been removed. This mean motion can be thought of as an orbit averaged motion. The Brouwer-Lyddane theory is used to obtain a first order analytic mapping between the osculating and mean orbit elements at any instance of time.[28,29] Using this theory, given any instantaneous osculating orbit elements, it is possible to compute the corresponding mean orbit elements without performing any averaging computation over time. This is attractive for spacecraft formation flying, where often it is not necessary to control the short or long term period motions of the relative orbit, but rather the focus is to avoid and counter the long-term drift caused by the secular motion.

Although all six orbit elements will vary with time, when mapping the osculating orbit elements to mean orbit elements, only three orbit elements are found to exhibit secular grow due to the J_2 gravitational influence. Let the parameter ϵ be defined as

$$\epsilon(a,e) = 3J_2\left(\frac{r_{eq}}{a(1-e^2)}\right)^2 \tag{52}$$

The mean element differential equations are given by.[25,30]

$$\dot{\boldsymbol{e}}_1(t) = \begin{cases} \dfrac{{\rm d}a}{{\rm d}t} &= 0 \\ \dfrac{{\rm d}e}{{\rm d}t} &= 0 \\ \dfrac{{\rm d}i}{{\rm d}t} &= 0 \end{cases} \tag{53a}$$

$$\dot{\boldsymbol{e}}_2(t) = \begin{cases} \dfrac{{\rm d}\Omega}{{\rm d}t} &= -\dfrac{\epsilon(a,e)}{2}n\cos i \\ \dfrac{{\rm d}\omega}{{\rm d}t} &= \dfrac{\epsilon(a,e)}{4}n\left(5\cos^2 i - 1\right) \\ \dfrac{{\rm d}M_0}{{\rm d}t} &= \dfrac{\epsilon(a,e)}{4}n\,\eta\left(3\cos^2 i - 1\right) \end{cases} \tag{53b}$$

Unless noted otherwise, this section assumes that all orbit elements have been mapped into the mean element space. As such, only the secular J_2 induced motions are considered. Note the natural split into the orbit elements sets $\boldsymbol{e}_1 = \{a, e, i\}$ and $\boldsymbol{e}_2 = \{\Omega, \omega, M_0\}$ in the mean element differential equations in Eq. (53). Thus, while the mean element set $\boldsymbol{e}_2$ will experience secular drift due to the J_2 gravitational perturbation, the rate of drift is constant and solely determined by the invariant mean element set $\boldsymbol{e}_1$.

To predict the *mean* linearized relative motion using the orbit element difference expressions in Eqs. (41), the differential equations $\dot{\boldsymbol{e}}_2$ in Eqs. (53) could be analytically integrated with respect to time to yield the chief and deputy orbit element time histories $\boldsymbol{e}(t)$ and $\boldsymbol{e}_d(t)$ respectively. Note that only the three uncoupled orbit element difference differential equations $\{\delta\dot{\Omega}, \delta\dot{\omega}, \delta\dot{M}_0\}$ need to be integrated, since the mean $\{a, e, i\}$ elements to not vary under the influence of the J_2 gravitational attraction. However, to find the *osculating* linearized relative motion, all twelve differential equations for the chief and deputy osculating orbit elements would have to be solved. Let us focus on computing the mean relative motion between satellites. Since $\dot{\boldsymbol{e}}_2$ is constant (see Eq. (53b)), the differential equations $\{\delta\dot{\Omega}, \delta\dot{\omega}, \delta\dot{M}_0\}$ are trivially solved to yield $\{\delta\Omega(t), \delta\omega(t), \delta M_0(t)\}$. However, to use these time dependent orbit element differences in the linearized relative motion solution in Eq. (41), it is still necessary to solve Kepler's equation at each time step to map the time state t into an equivalent true anomaly angle f.

The following development will illustrate how this can be avoided to yield a complete analytical solution of the linearized relative motion (in mean element space) using the true anomaly angle f as the independent variable. Taking the first variation of $\dot{\boldsymbol{e}}_2$, we are able to estimate how the

small orbit element differences $\delta\boldsymbol{e}_1 = \{\delta a, \delta e, \delta i\}$ will affect the orbit element difference rates $\delta\dot{\boldsymbol{e}}_2 = \{\delta\dot{\Omega}, \delta\dot{\omega}, \delta\dot{M}_0\}$.

$$\delta\dot{\Omega}(t) = \epsilon\, n \left(\frac{7}{4}\cos i\frac{\delta a}{a} - 2\frac{e}{\eta^2}\cos i\,\delta e + \frac{1}{2}\sin i\,\delta i\right) \tag{54a}$$

$$\begin{aligned}\delta\dot{\omega}(t) = \epsilon\, n\Big(&-\frac{7}{8}(5\cos^2 i - 1)\frac{\delta a}{a} \\ &+ \frac{e}{\eta^2}(5\cos^2 i - 1)\delta e - \frac{5}{4}\sin(2i)\,\delta i\Big)\end{aligned} \tag{54b}$$

$$\begin{aligned}\delta\dot{M}_0(t) = \epsilon\, n\Big(&-\frac{7}{8}\eta(3\cos^2 i - 1)\frac{\delta a}{a} \\ &+ \frac{3}{4}\frac{e}{\eta}(3\cos^2 i - 1)\delta e - \frac{3}{4}\eta\sin(2i)\,\delta i\Big)\end{aligned} \tag{54c}$$

Next, these differential equations are multiplied by $\mathrm{d}t/\mathrm{d}f$ in Eq. (18) to obtain $\delta\boldsymbol{e}_2'$.

$$\delta\Omega'(f) = \epsilon\delta\kappa_\Omega\frac{\eta^3}{(1+e\cos f)^2} \tag{55a}$$

$$\delta\omega'(f) = \epsilon\delta\kappa_\omega\frac{\eta^3}{(1+e\cos f)^2} \tag{55b}$$

$$\delta M_0'(f) = \epsilon\delta\kappa_M\frac{\eta^3}{(1+e\cos f)^2} \tag{55c}$$

with

$$\begin{aligned}\delta\kappa_\Omega &= \Big(\frac{7}{4}\cos i\frac{\delta a}{a} - 2\frac{e}{\eta^2}\cos i\,\delta e + \frac{1}{2}\sin i\,\delta i\Big) \\ \delta\kappa_\omega &= \Big(-\frac{7}{8}(5\cos^2 i - 1)\frac{\delta a}{a} + \frac{e}{\eta^2}(5\cos^2 i - 1)\delta e \\ &\quad - \frac{5}{4}\sin(2i)\,\delta i\Big) \\ \delta\kappa_M &= \Big(-\frac{7}{8}\eta(3\cos^2 i - 1)\frac{\delta a}{a} + \frac{3}{4}\frac{e}{\eta}(3\cos^2 i - 1)\delta e \\ &\quad - \frac{3}{4}\eta\sin(2i)\,\delta i\Big)\end{aligned}$$

Note that the terms $\delta\kappa_\Omega$, $\delta\kappa_\omega$ and $\delta\kappa_M$ are constants since the mean δa, δe and δi orbit element differences to not vary under the influence of the J_2 gravitational perturbation. Making use of the integral expression in Eq. (20), these differential equations are integrated with respect to the true anomaly angle f to yield:

$$\delta\Omega(f) = \delta\Omega(f_0) + \epsilon\,\delta\kappa_\Omega(M(f) - M_0) \tag{56a}$$

$$\delta\omega(f) = \delta\omega(f_0) + \epsilon\,\delta\kappa_\omega(M(f) - M_0) \tag{56b}$$

$$\delta M_0(f) = \delta M_0(f_0) + \epsilon\,\delta\kappa_M(M(f) - M_0) \tag{56c}$$

The current mean anomaly difference $\delta M(f)$ is found by substituting the $\delta M_0(f)$ into Eq. (21). With these analytic solutions to the mean $\delta\Omega(f)$, $\delta\omega(f)$ and $\delta M(f)$ behavior, using Eq. (41) we have an analytic solution to the mean linearized relative orbit motion with the J_2 gravitational perturbation included. If we assume that the chief orbit is only weakly linear, then the terms $\delta\kappa_\Omega$, $\delta\kappa_\omega$ and $\delta\kappa_M$ reduce to

$$\delta\kappa_\Omega = \frac{7}{4}\cos i\frac{\delta a}{a} - 2e\cos i\,\delta e + \frac{1}{2}\sin i\,\delta i \tag{57}$$

$$\begin{aligned}\delta\kappa_\omega = &-\frac{7}{8}(5\cos^2 i - 1)\frac{\delta a}{a} + e(5\cos^2 i - 1)\delta e \\ &- \frac{5}{4}\sin(2i)\,\delta i\end{aligned} \tag{58}$$

$$\begin{aligned}\delta\kappa_M = &-\frac{7}{8}\eta(3\cos^2 i - 1)\frac{\delta a}{a} + \frac{3}{4}e(3\cos^2 i - 1)\delta e \\ &- \frac{3}{4}\eta\sin(2i)\,\delta i\end{aligned} \tag{59}$$

If the chief orbit is near circular, then all terms containing e are dropped leading to the simplified terms:

$$\delta\kappa_\Omega = \frac{7}{4}\cos i\frac{\delta a}{a} + \frac{1}{2}\sin i\,\delta i \tag{60}$$

$$\delta\kappa_\omega = -\frac{7}{8}(5\cos^2 i - 1)\frac{\delta a}{a} - \frac{5}{4}\sin(2i)\,\delta i \tag{61}$$

$$\delta\kappa_M = -\frac{7}{8}\eta(3\cos^2 i - 1)\frac{\delta a}{a} - \frac{3}{4}\eta\sin(2i)\,\delta i \tag{62}$$

Note that this elegant analytical solution to the orbit element differences $\delta\boldsymbol{e}(f)$ is only possible since for the mean motion the $\delta\dot{\boldsymbol{e}}_2(t)$ rates only depend on the constant mean $\boldsymbol{e}_1$ and $\delta\boldsymbol{e}_1$ parameters. When computing the $\delta\boldsymbol{e}_2'(f)$ rates the expressions do depend on the independent variable f, but are still analytically integrable. In comparison, to find the osculating linearized relative motion, it is necessary to numerical integrate the 12 orbit element differential equations $\boldsymbol{e}'(f)$ and $\boldsymbol{e}_d'(f)$ for the chief and deputy satellites to obtain the required $\delta\boldsymbol{e}(f)$ values.

Numerical Simulations

The following numerical simulations verify that the relative motion approximation in Eqs. (35), (46) and (50) do indeed predict the spacecraft formation geometry. These simulations also illustrate the accuracy at which these simplified linearized solutions are valid. Let the chief orbit be given by the orbit elements shown in Table 1.

Table 1 Chief Orbit Elements

Orbit Elements	Value	Units
a	7555	km
e	0.03 or 0.13	
i	48.0	deg
Ω	20.0	deg
ω	10.0	deg
M_0	0.0	deg

The relative orbits are studied for two different chief eccentricities. For the relative orbits studied, the ratio ρ/r is about 0.003. The smaller of the two eccentricities considered is already an order of magnitude larger than this, while the second eccentricity is even larger again. The numerical simulations show that the small eccentricity assumption (i.e. retaining terms in e but dropping higher order terms in e) will still yield a reasonable relative orbit prediction for $e = 0.03$, even though it is larger than the small term ρ/r. The orbit element differences which define the relative orbit are given in Table 2. Since these simulations assume Keplerian motion of the satellites, the semi-major axis difference δa must be zero to achieve a bounded relative motion.

Table 2 Orbit Element Differences Defining the Spacecraft Formation Geometry

Orbit Elements	Value	Units
δa	0	km
δe	0.00095316	
δi	0.0060	deg
$\delta\Omega$	0.100	deg
$\delta\omega$	0.100	deg
δM_0	-0.100	deg

For example, for the $e = 0.13$ case these orbit element differences were chosen assuming the relative orbit is to have an angular along-track offset of 0.060777 degrees, a sinusoidal along-track angular motion of 0.027435 degrees and an angular out-of-plane motion of 0.074556 degrees. Thus, using Eq. (41a), δM_0, $\delta\omega$ and $\delta\Omega$ are chosen such that

$$\left(1 + \frac{e^2}{2}\right)\frac{\delta M_0}{\eta^3} + \delta\omega + \cos i\delta\Omega = 0.060777 \text{ degrees}$$

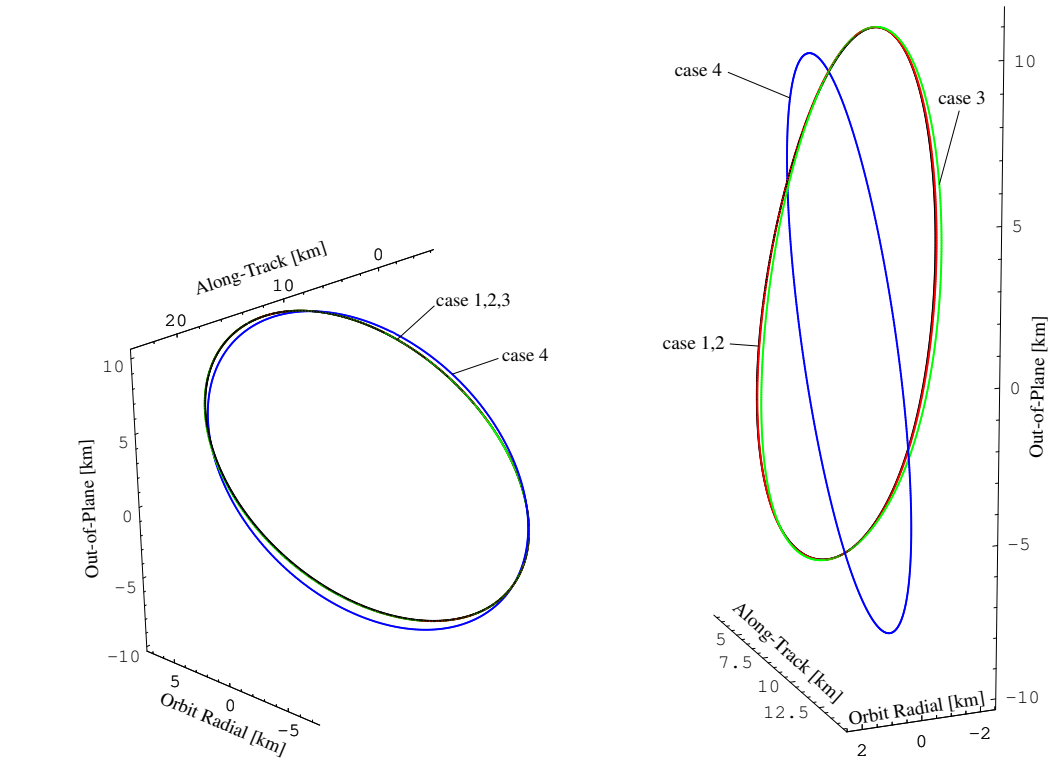

a) Relative Orbits in Hill Frame for $e = 0.03$

b) Relative Orbits in Hill Frame for $e = 0.13$

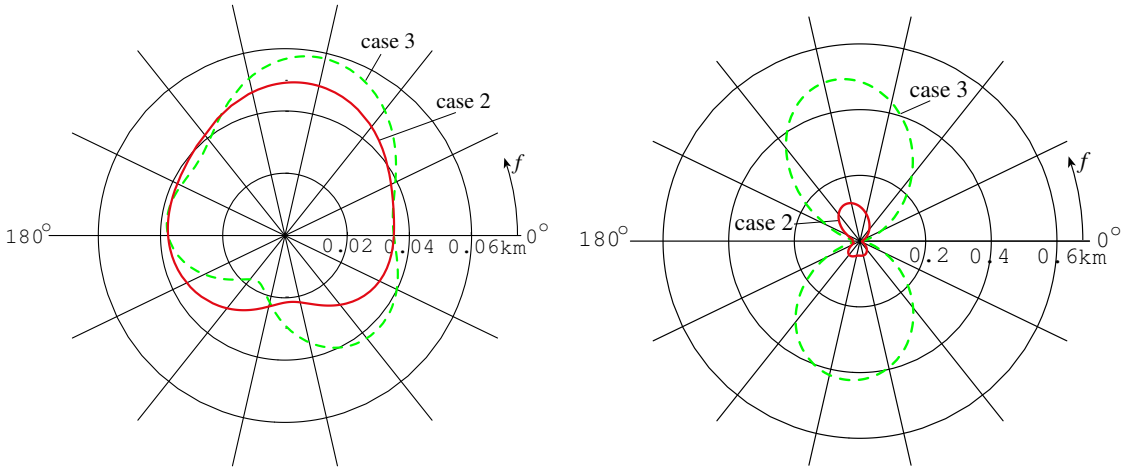

c) RMS Relative Orbit Error in kilometers vs. Chief True Anomaly Angle f for $e = 0.03$

d) RMS Relative Orbit Error in kilometers vs. Chief True Anomaly Angle f for $e = 0.13$

Fig. 3 Comparison of the Linearized Relative Orbit Solutions for Cases 1–4 with $e = 0.03$ and $e = 0.13$.

Clearly this choice in δM_0, $\delta\omega$ and $\delta\Omega$ is not unique. Other combinations would yield the same angular offset. The eccentricity difference δe is chosen using Eq. (41b) such that

$$\frac{2}{\eta^2}\sqrt{\frac{e^2\delta M_0^2}{\eta^2} + \delta e^2} = 0.027435 \text{ degrees}$$

Finally, the inclination angle difference is chosen using Eq. (41c) such that

$$\sqrt{\delta i^2 + \sin^2 i\,\delta\Omega^2} = 0.074556 \text{ degrees}$$

The following figures compare the relative orbit motion for four different cases. Case 1 is the relative motion that will result using the true nonlinear equations of motion. Case 2 uses the dimensional linearized analytical relative orbit solution in Eq. (35). The only assumption that has been made here is that the ratio between the relative orbit radius ρ and the inertial chief orbit radius r is small and terms involving ρ/r have been dropped. Case 3 assumes that the chief orbit eccentricity is small, but not near zero. The relative orbit motion is described through Eq. (46). Case 4 uses Eq. (50) which assumes that the chief orbit is near-circular and that e is very close to zero. Case 4 is not included here to suggest that a circular orbit assumption should be made when the chief orbit is clearly eccentric. The circular chief orbit assumption case is included to provide a relative comparison illustrating the extent of the eccentricity effect.

The resulting relative orbit motion is illustrated in Figure 3. Figures 3(a) and 3(b) show the three-dimensional relative orbits for cases 1 through 4 as seen by the rotating Hill reference frame. The relative orbit radii vary between 10 and 20 kilometers. When $e = 0.03$, note that the relative orbits for cases 1–3 are virtually indistinguishable. Only the relative orbit prediction assuming a circular orbit (case 4) has a clearly distinct motion. Studying Figure 3(b) with $e = 0.13$, the case 2 relative orbit is still indistinguishable on this scale from the true relative motion in case 1. With this

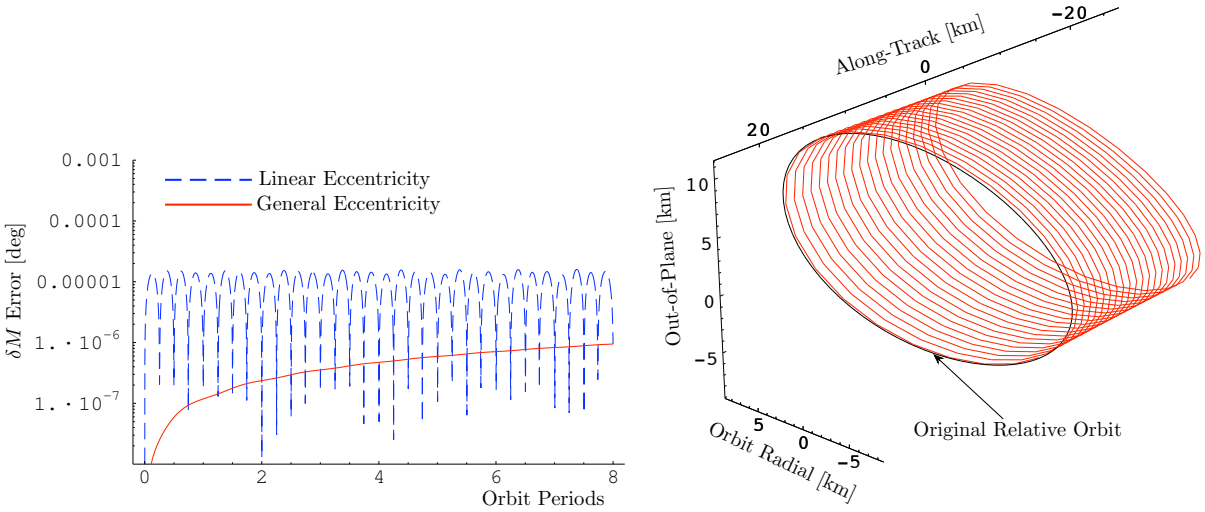

a) Mean Anomaly Difference Approximation Error **b)** Hill Orbit Frame View for Parameter Set 1 with Keplerian Orbits

Fig. 4 Mean Anomaly Difference Drift Predictions with Keplerian Orbits.

larger eccentricity the relative motion predicted in case 3 (dropping higher order terms in e) does show some visible departure from the true relative motion. As expected, the circular chief orbit assumption (case 4) yields a very poor prediction of the relative orbit motion.

In Figures 3(c) and 3(d) the RMS relative orbit errors are shown in polar plots versus the chief orbit true anomaly. For the $e = 0.03$ simulations, the relative orbit errors for case 2 lie between 20 and 40 meters. Since the relative orbit radius is roughly 10 kilometers, this corresponds to a 0.2–0.4 percent relative motion error. The RMS relative motion error for case three is only marginally worse. As was discussed earlier, dropping the higher order e terms should begin to have a noticeable affect on the relative motion errors. For the $e = 0.13$ simulations, the relative motion errors for case 2 lie between 50 and 100 meters (roughly 0.5–1.0 percent errors). However, dropping the higher order e terms in case 3 has a very noticeable effect with the relative motion errors growing as large as 500 meters (about 5.0 percent error).

To illustrate the accuracy of the linearized mean anomaly drift prediction in Eq. (21), the orbit elements in Table 1 and the orbit element difference in Table 2 are used, except for the semi-major axis difference δa being 0.1 kilometers in this case. The chief eccentricity is 0.13.

Figure 4(a) compares the mean anomaly drift approximation errors of Eq. (21) (solid line) and Eq. (24) (dashed line) relative to the true nonlinear solution on a logarithmic scale over 8 orbits. While the small eccentricity approximation does yield noticeably worse predictions, over a few orbits these errors are all still very small in magnitude. The corresponding relative orbit is illustrated in Figure 4(b).

Conclusion

Analytical linearized relative orbit descriptions are provided for several types of chief orbit eccentricities, where orbit element differences are chosen to define the relative orbit geometry. The relative orbit motion between a deputy and chief satellite is expressed with the true anomaly angle as the independent variable. With these linearized relative motion solutions, it is trivial to estimate what the geometric effect of changing a particular orbit element difference will be. For the bounded relative motion case, the relative orbit solutions are written such that their secular offset and sinusoidal motions are clearly separated. As such, it is easy to see what the offsets and sinusoidal amplitudes will be for a given set of orbit element differences in the orbit radial, along-track and out-of-plane motion. Orbit element differences have the advantage that they are constants of the Keplerian two-body solution if the mean anomaly difference is selected as the relative anomaly measure and the semi-major axis difference is zero. If the bounded relative orbit constraint is not satisfied, or there are other perturbations present such as the J_2 gravitational perturbations, then some or all of the orbit element differences will vary slowly with time. The presented analytical solutions in terms of the orbit element differences are still valid. However, care must be taken to treat the appropriate orbit element differences as time varying. Analytical orbit element difference drift equations are provided for the non-zero δa case and for studying the mean relative orbit motion under the gravitational J_2 influence. To account for more general orbit perturbations, the corresponding orbit element difference differential equations would need to be numerically solved to use the presented relative orbit descriptions.

Acknowledgment

I would like to thank Prof. K. T. Alfriend for the fruitful discussions that led to an enhanced version of this paper.

References

[1]Kechichian, J. A., "The Analysis of the Relative Motion in General Elliptic Orbit with Respect to a Dragging and Precessing Coordinate Frame," *AAS/AIAA Astrodynamics Specialist Conference*, Sun Valley, Idaho, August 1997, Paper No. 97-733.

[2]Queiroz, M. S. D., Kapila, V., and Yan, Q., "Nonlinear Control of Multiple Spacecraft Formation Flying," *Proceedings of AIAA Guidance, Navigation, and Control Conference*, Portland, OR, Aug. 1999, Paper No. AIAA 99–4270.

[3]Sedwick, R., Miller, D., and Kong, E., "Mitigation of Differential Perturbations in Clusters of Formation Flying Satellites," *AAS/AIAA Space Flight Mechanics Meeting*, February 1999, Paper No. AAS 99-124.

[4]Schaub, H. and Alfriend, K. T., "J_2 Invariant Reference Orbits for Spacecraft Formations," *Celestial Mechanics and Dynamical Astronomy*, Vol. 79, No. 2, 2001, pp. 77–95.

[5]Alfriend, K. T. and Schaub, H., "Dynamics and Control of Spacecraft Formations: Challenges and Some Solutions," *Journal of the Astronautical Sciences*, Vol. 48, No. 2 and 3, April–Sept. 2000, pp. 249–267.

[6]Garrison, J. L., Gardner, T. G., and Axelrad, P., "Relative Motion in Highly Elliptic Orbits," *AAS/AIAA Space Flight Mechanics Meeting*, Albuquerque, NM, Feb. 1995, Paper No. 95-194.

[7]Chichka, D. F., "Satellite Cluster with Constant Apparent Distribution," *Journal of Guidance, Control and Dynamics*, Vol. 24, No. 1, Jan.–Feb. 2001, pp. 117–122.

[8]Hughes, S. P. and Hall, C. D., "Optimal Configurations of Rotating Spacecraft Formations," *Journal of the Astronautical Sciences*, Vol. 48, No. 2 and 3, April–Sept. 2000, pp. 225–247.

[9]Schaub, H., Vadali, S. R., and Alfriend, K. T., "Spacecraft Formation Flying Control Using Mean Orbit Elements," *Journal of the Astronautical Sciences*, Vol. 48, No. 1, 2000, pp. 69–87.

[10]Tan, Z., Bainum, P. M., and Strong, A., "The Implementation of Maintaining Constant Distance Between Satellites in Elliptic Orbits," *AAS Spaceflight Mechanics Meeting*, Clearwater, Florida, Jan. 2000, Paper No. 00-141.

[11]Schaub, H. and Alfriend, K. T., "Impulsive Feedback Control to Establish Specific Mean Orbit Elements of Spacecraft Formations," *Journal of Guidance, Control and Dynamics*, Vol. 24, No. 4, July–Aug. 2001, pp. 739–745.

[12]Schaub, H. and Alfriend, K. T., "Hybrid Cartesian and Orbit Element Feedback Law for Formation Flying Spacecraft," *Journal of Guidance, Control and Dynamics*, Vol. 25, No. 2, March–April 2002, pp. 387–393.

[13]Naasz, B. J., Karlgaard, C. D., and Hall, C. D., "Application of Several Control Techniques for the Ionospheric Observation Nanosatellite Formation," AAS/AIAA Space Flight Mechanics Meeting, San Antonio, TX, Jan. 2002, Paper No. AAS 02-188.

[14]Melton, R. G., "Time-Explicit Representation of Relative Motion Between Elliptical Orbits," *Journal of Guidance, Control, and Dynamics*, Vol. 23, No. 4, 2000, pp. 604–610.

[15]Tschauner, J. and Hempel, P., "Rendezvous zu einem in Elliptischer Bahn Umlaufenden Ziel," *Astronautica Acta*, Vol. 11, No. 5, 1965, pp. 104–109.

[16]Kechichian, J. and Kelly, T., "Analytical Solution of Perturbed Motion in Near-Circular Orbit Due to J2, J3 Earth Zonal Harmonics in Rotating and Inertial Cartesian Reference Frames," *AIAA 27th Aerospace Sciences Meeting*, Reno, Nevada, January 1989, Paper No. 89-0352.

[17]Carter, T. E., "State Transition Matrix for Terminal Rendezvous Studies: Brief Survey and New Example," *Journal of Guidance, Control and Dynamics*, Vol. 31, No. 1, 1998, pp. 148–155.

[18]Gim, D.-W. and Alfriend, K. T., "The State Transition Matrix of Relative Motion for the Perturbed Non-Circular Reference Orbit," *AAS/AIAA Space Flight Mechanics Meeting*, Santa Barbara, CA, Feb. 2001, Paper No. 01-222.

[19]Broucke, R. A., "A Solution of the Elliptic Rendezvous Problem with the Time as Independent Variable," *AAS/AIAA Space Flight Mechanics Meeting*, San Antonio, TX, January 2002, Paper No. AAS 02-144.

[20]Inalhan, G., Tillerson, M., and How, J. P., "Relative Dynamics & Control of Spacecraft Formations in Eccentric Orbits," *Journal of Guidance, Control and Dynamics*, Vol. 25, No. 1, Jan.–Feb. 2002, pp. 48–59.

[21]Alfriend, K. T., Schaub, H., and Gim, D.-W., "Gravitational Perturbations, Nonlinearity and Circular Orbit Assumption Effect on Formation Flying Control Strategies," *AAS Guidance and Control Conference*, Breckenridge, CO, February 2000, Paper No. AAS 00-012.

[22]Hill, G. W., "Researches in the Lunar Theory," *American Journal of Mathematics*, Vol. 1, No. 1, 1878, pp. 5–26.

[23]DeVries, J. P., "Elliptic Elements in Terms of Small Increments of Position and Velocity Components," *AIAA Journal*, Vol. 1, No. 9, Nov. 1963, pp. 2626–2629.

[24]Clohessy, W. H. and Wiltshire, R. S., "Terminal Guidance System for Satellite Rendezvous," *Journal of the Aerospace Sciences*, Vol. 27, No. 9, Sept. 1960, pp. 653–658.

[25]Schaub, H. and Junkins, J. L., *Analytical Mechanics of Space Systems*, AIAA Education Series, Reston, VA, 2003.

[26]Beyer, W. H., *Standard Mathematical Tables*, CRC Press, Inc., West Palm Beach, Fl., 1974.

[27]Hughes, S. P. and Mailhe, L. M., "A Preliminary Formation Flying Orbit Dynamics Analysis for Leonardo-BRDF," *IEEE Aerospace Conference*, Big Sky, Montana, March 11–17 2001, Paper No. 905.

[28]Brouwer, D., "Solution of the Problem of Artificial Satellite Theory Without Drag," *The Astronomical Journal*, Vol. 64, No. 1274, 1959, pp. 378–397.

[29]Lyddane, R. H., "Small Eccentricities or Inclinations in the Brouwer Theory of the Artificial Satellite," *The Astronomical Journal*, Vol. 68, No. 8, October 1963, pp. 555–558.

[30]Battin, R. H., *An Introduction to the Mathematics and Methods of Astrodynamics*, AIAA Education Series, New York, 1987.